Albero V, Espinós A, Romero ML, Wang YC, Renaud C, Schaumann P, Nigro E. Interaction diagram based method for fire resistance design of eccentrically loaded concrete-filled steel tubular columns. Thin-Walled Structures 2018; 130:641-651. doi: https://doi.org/10.1016/j.tws.2018.06.017

# Interaction diagram based method for fire resistance design of eccentrically loaded concrete-filled steel tubular columns

V. Albero [a], A. Espinós [a,*], M. L. Romero [a], Y. C. Wang [b], C. Renaud [c], P. Schaumann[d], E. Nigro[e]

[a] *Instituto de Ciencia y Tecnología del Hormigón (ICITECH), Universitat Politècnica de València, Valencia, Spain*
[b] *School of Mechanical, Aerospace and Civil Engineering, University of Manchester, United Kingdom*
[c] *Centre Technique Industriel de la Construction Métallique (CTICM), Saint Aubin, France*
[d] *Institute for Steel Construction, Leibniz Universität Hannover, Hannover, Germany*
[e] *Department of Structures for Engineering and Architecture, School of Engineering, University of Naples Federico II, Naples, Italy*
* *Corresponding author. e-mail address: aespinos@mes.upv.es*

## ABSTRACT

Previous investigations have highlighted that the current design method in Annex H of EN 1994-1-2 for the calculation of fire resistance of slender concrete-filled steel tubular (CFST) columns was unsafe, which led to the appointment of a Project Team (SC4.T4) by the European Committee for Standardization (CEN) to develop a new Annex H in EN1994-1-2 to replace the existing one. This paper presents the outcome of the Project Team, a new simplified fire design method for CFST columns, focusing in particular on eccentrically loaded columns for which there had been no systematic research. An extensive parametric study consisting of 5046 analysis cases has been carried out, covering all the practical ranges of application of CFST columns. The method accounts for minor and major axis eccentricities with large eccentricities up to $e/D = 1$. Different bending moment diagrams, ranging from single curvature to double curve bending, were considered. The proposed new design method is in line with the cold design method in EN1994-1-1 and achieves the criteria of acceptance for safe and accurate design of structures in fire which were set by the CEN/TC250 Horizontal Group Fire.

Albero V, Espinós A, Romero ML, Wang YC, Renaud C, Schaumann P, Nigro E. Interaction diagram based method for fire resistance design of eccentrically loaded concrete-filled steel tubular columns. Thin-Walled Structures 2018; 130:641-651. doi: https://doi.org/10.1016/j.tws.2018.06.017

Keywords*: Concrete-filled steel tubular columns; fire resistance; eccentric load; simplified design method; numerical analysis; parametric studies; Eurocode 4*

**NOTATION**

| | |
|---|---|
| $A_{i,\theta}$ | cross-sectional area of the part *i* of the composite section at temperature $\theta$ |
| $A_m$ / V | section factor accounting for steel and concrete |
| $A_{sn}$ | area of reinforcing bars within the region of depth $h_n$ |
| $B$ | width of the square section or smaller outer dimension of elliptical or rectangular section |
| CFST | Concrete-Filled Steel Tube |
| CHS | Circular Hollow Section |
| $D$ | outer diameter of circular section |
| $e$ | eccentricity of loading |
| $e_{imp}$ | eccentricity from geometrical imperfection |
| $E_{i,\theta}$ | modulus of elasticity of material *i* at temperature $\theta$ |
| $(EI)_{fi,eff}$ | effective flexural stiffness for calculation of relative slenderness in the fire situation |
| $(EI)_{fi,eff,II}$ | effective flexural stiffness for use in second order analysis in the fire situation |
| EHS | Elliptical Hollow Section |
| $f_c$ | compressive cylinder strength of concrete at room temperature |
| $f_s$ | yield strength of reinforcing steel at room temperature |
| $f_y$ | yield strength of structural steel at room temperature |
| $H$ | larger outer dimension of elliptical or rectangular section |
| $I_{i,\theta}$ | second moment of area of part *i* of the cross-section at temperature $\theta$ |
| $K_{e,II}$, $K_0$ | correction factors for calculating the second order flexural stiffness at room temperature |
| $K_\theta$ | elevated temperature correction factor for calculating the second order flexural stiffness |
| $k_{i,\theta}$ | reduction factor for a material property at elevated temperature $\theta$ |
| $k_{fi}$ | amplification factor for second order effects at elevated temperature $\theta$ |

$L$ nominal length of column

$l_\theta$ buckling length of column in the fire situation

$M_{fi,Ed}$ design bending moment applied to the composite section in the fire situation

$M_{fi,1,Ed}$ first order bending moment in the fire situation

$M_{fi,2,Ed}$ second order bending moment in the fire situation

$M_{fi,pl,N,Rd}$ design value of the plastic resistance moment of the composite section in the fire situation, taking into account the compressive normal force

$M_{fi,pl,Rd}$ design value of the plastic resistance moment of the composite section in the fire situation without compressive force

$N_{fi,cr}$ elastic critical normal force in the fire situation

$N_{fi,cr,eff}$ elastic critical normal force corresponding to the effective flexural stiffness in the fire situation

$N_{fi,Ed}$ design value of the compressive normal force in the fire situation

$N_{fi,pl,Rd}$ design value of the plastic resistance of the composite section to compressive normal force in the fire situation

$r$ end moment ratio

RHS Rectangular Hollow Section

SHS Square Hollow Section

$t$ steel tube wall thickness

$t_{fi}$ fire exposure time

$W_{pa}$ plastic section modulus of steel

$W_{pan}$ plastic section modulus of the steel region with depth $2h_n$

$W_{pcn}$ plastic section modulus of the concrete region with depth $2h_n$

$W_{pc}$ plastic section modulus of concrete

$W_{ps}$ plastic section modulus of reinforcing bars

$W_{psn}$ plastic section modulus of the reinforcing bars within depth $2h_n$

$\alpha_M$ safety factor for reducing the M-N interaction curve

$\beta$ equivalent moment factor

$\beta_i$ coefficients for evaluating the equivalent temperature of reinforcing bars

$\theta$ temperature

$\theta_{i,eq}$ equivalent temperature of part i of the cross-section

$\bar{\lambda}$ relative slenderness at room temperature

$\bar{\lambda}_\theta$ relative slenderness in the fire situation

$\varphi_{i,\theta}$ stiffness reduction coefficient to make allowance for the effect of thermal stresses

$\rho_s$ percentage of reinforcement

$\mu$ axial load level

$\mu_{fi,d}$ ratio of available bending resistance under compression to bending resistance without compression in the fire situation

# 1 INTRODUCTION

Concrete-filled steel tubular columns are an attractive structural solution but their applications are hampered by the lack of a safe, accurate and widely applicable simplified calculation method for fire design. At present, there are two methods in Europe. In the main part of Eurocode 4 Part 1-2 (EN1994-1-2 [1]), a general calculation method is provided to estimate the buckling resistance of composite columns in braced frames at elevated temperatures. However, this method is only applicable to axially loaded CFST columns without any bending moment. If there are bending moments in the CFST column, which is usually the case in practice, the existing Eurocode method is presented in Annex H of EN 1994-1-2 [1]. However, despite complexity in implementation, this method lacks a robust technical base, and has been demonstrated to be unsafe for slender columns [2, 3], leading to an addenda approved by CEN/TC250/SC4 [4] which limits the maximum relative slenderness to 0.5. Also, this method is only valid for CHS and SHS columns, being out of scope for other geometries used in practice, such as rectangular or elliptical sections. This method is not allowed in many countries such as France [5, 6], Finland [7], the United Kingdom [8] and Spain [9, 10], where it has been replaced by alternative design rules.

Other methods exist worldwide for the evaluation of fire resistance of CFST columns, such as those used in North America [11], China [12] or Japan [13], but they all have severe limitations in their scopes of application.

This unsatisfactory situation has led the European Committee for Standardization (CEN) to appoint a Project Team to develop a new simplified fire resistance design method for CFST columns. Prior to this Project Team's activities, the authors of this paper completed the European RFCS funded research project entitled "Fire Resistance of Innovative and Slender Concrete Filled Tubular Composite Columns" (FRISCC) [14]. As a result of this project, a

simplified method was developed. A key contribution of the simplified method is to assume that the effects of non-uniform temperature in the CFST cross-section can be represented by an equivalent uniform temperature for each of the different components (steel tube, concrete infill, reinforcement) of the CFST cross-section. Although the FRISCC project also proposed a calculation method for CFST columns under eccentric loading, the method was quite tedious to apply and was for single curvature only.

For CFST columns with bending moments, the UK design method, based on the work of Wang and Orton [15], recommends using the cold design method for composite columns in Eurocode EN 1994-1-1 [16]. Thus, if the equivalent uniform temperatures of [16] are used in combination with the recommendation of Wang and Orton [15], the fire resistance calculation for CFST columns is simplified into a cold design problem, with modifications to use elevated temperature properties being the main change. The CEN Project Team SC4.T4 considered this attractive, because it has made the cold and fire resistance design of CFST columns consistent and has made it very easy to calculate the fire resistance of CFST columns.

However, for eccentrically loaded CFST columns with different bending moment distributions, the proposed new method did not have sufficient data for its validation. This is the subject of the present paper. This paper will first present the new simplified method and then use the results of an extensive numerical study to check its accuracy and acceptance.

## 2 PROPOSED SIMPLIFIED METHOD

### 2.1 Equivalent temperatures and flexural stiffness at elevated temperatures

In this new method, instead of dealing with non-uniform temperatures in the different components of CFST columns, equations are provided to calculate the equivalent uniform

temperatures for each of the CFST components (steel tube, concrete core, reinforcement), as schematized in Fig. 1. The equivalent uniform temperatures can be calculated as follows.

For the concrete core ($\theta_{c,eq}$):

$$\theta_{c,eq} = 81.8 - 5.05 \cdot t_{fi} + 0.003 \cdot t_{fi}^{\,2} - 15.07 A_m / V + 0.3 (A_m / V)^2 - 0.88 \cdot t_{fi} \cdot A_m / V + \\ + 7.43 \cdot t_{fi}^{\,0.842} \cdot \left( A_m / V \right)^{0.714} \quad (1)$$

For the steel tube ($\theta_{a,eq}$):

$$\theta_{a,eq} = -824.67 - 5.58 \cdot t_{fi} + 0.007 \cdot t_{fi}^{\,2} - 0.01 \cdot t_{fi} \cdot A_m / V + 645.08 \cdot t_{fi}^{\,0.269} \cdot \left( A_m / V \right)^{0.017} \quad (2)$$

For the reinforcing bars ($\theta_{s,eq}$):

$$\theta_{s,eq} = \beta_3 \cdot \left( t_{fi} / u_s^2 \right)^3 + \beta_2 \cdot \left( t_{fi} / u_s^2 \right)^2 + \beta_1 \cdot \left( t_{fi} / u_s^2 \right) + \beta_0 \quad (3)$$

where the $\beta_i$ coefficients depend on the CFST section shape and concrete cover, and are given in [16].

By using the equivalent uniform temperatures, a heated CFST column is converted into a cold CFST column with different material properties, except for the necessity to introduce modification factors to the flexural stiffness values of the different components of the CFST column due to the effects of thermal stress. Therefore, the flexural stiffness of a composite CFST column is calculated as:

$$(EI)_{fi,eff} = \varphi_{a,\theta} \cdot E_a(\theta_{a,eq}) I_a + \varphi_{s,\theta} \cdot E_s(\theta_{s,eq}) I_s + \varphi_{c,\theta} \cdot E_c(\theta_{c,eq}) I_c \quad (4)$$

and the flexural stiffness reduction coefficients are obtained as follows (based on the authors' previous investigations [16]).

Steel tube:

- CHS: $\varphi_{a,\theta} = 0.75 - 0.023 \cdot \left( A_m / V \right)$
- SHS: $\varphi_{a,\theta} = 0.15 - 0.001 \cdot \left( A_m / V \right)$

- RHS and EHS: $\varphi_{a,\theta} = 0.012 \cdot (l_\theta / \mathrm{B})_*$

* when eccentricity is applied for bending about the major axis, *B* should be replaced by *H*

Concrete core: $\varphi_{c,\theta} = 1.2$ (used in combination with the secant modulus)

Reinforcing bars:

- CHS and SHS: $\varphi_{s,\theta} = 0.8 - 0.002 \cdot t_{fi}$
- RHS: $\varphi_{s,\theta} = 0.7$
- EHS: $\varphi_{s,\theta} = 0.95$

## 2.2 Proposed method for eccentric loading

The same method as for cold design is proposed for fire design, but with some modifications. These are explained in this section.

Second order analysis is used in the cold design method, so the design bending moment is obtained by magnifying the applied first order bending moment $\left(M_{fi,1,Ed}\right)$ to account for second order effects $\left(M_{fi,2,Ed}\right)$. In turn, the first order bending moment can be expressed as the addition of the moment from eccentricity $\left(N_{fi,Ed} \cdot e\right)$ and that obtained from the maximum geometric imperfection $\left(N_{fi,Ed} \cdot e_{imp}\right)$:

$$M_{fi,2,Ed} = k_{fi} \cdot M_{fi,1,Ed} = k_{fi} \cdot \left(e + e_{imp}\right) N_{fi,Ed} \tag{5}$$

where the amplification factor $k_{fi}$ in the fire situation is defined as follows:

$$k_{fi} = \frac{\beta}{1 - \dfrac{N_{fi,Ed}}{N_{fi,cr,eff}}} \tag{6}$$

in which

$N_{fi,Ed}$ is the design axial load in the fire situation;

$\beta$ is an equivalent moment factor given in EN 1994-1-1 [17] Table 6.4, which takes into account moment distribution;

$N_{fi,cr,eff}$ is the critical normal force at elevated temperatures, which is a function of the second order effective flexural stiffness and the effective length of the column, both in fire, and can be calculated as:

$$N_{fi,cr,eff} = \frac{\pi^2 (EI)_{fi,eff,II}}{l_\theta^2} \tag{7}$$

The effective flexural stiffness of the column for second order analysis at elevated temperatures, $(EI)_{fi,eff,II}$, represents the global behaviour of the column taking into account the second-order effects in fire.

Using the same format as in the cold design method in EN 1994-1-1 [17] and taking into consideration the elevated temperature flexural stiffness, equation (4), the effective flexural stiffness $(EI)_{fi,eff,II}$ for second order analysis in the fire situation is expressed as follows:

$$(EI)_{\mathrm{fi,eff,II}} = K_\theta \cdot K_o \cdot \left[ \varphi_{a,\theta} \cdot E_a(\theta_{a,eq}) I_a + \varphi_{\mathrm{s},\theta} \cdot E_s(\theta_{\mathrm{s},eq}) I_s + K_{e,II} \cdot \varphi_{\mathrm{c},\theta} \cdot E_c(\theta_{\mathrm{c},eq}) I_c \right] \tag{8}$$

For cold design, $K_o = 0.9$ and $K_{e,II} = 0.5$. For fire design, an additional coefficient $(K_\theta)$ is proposed to take into account the influence of thermal stress at elevated temperatures on second-order effects.

For any column, the first order bending moment $(M_{fi,1,Ed})$ can be obtained from the applied axial load $(N_{fi,Ed})$ and the given eccentricity. Likewise, the available bending resistance for the second order bending moment $(M_{fi,2,Ed} = \mu_{fi,d} \cdot M_{fi,pl,Rd})$ under the given design axial load $(N_{fi,Ed})$ can be computed from the M-N interaction diagram of the cross-

section at elevated temperatures, see Fig. 2. From these two values, the stiffness correction factor at elevated temperatures $\left(K_\theta\right)$ can be calculated by performing the following steps in sequence:

a. The amplification factor is obtained:

$$k_{fi} = \frac{M_{fi,2,Ed}}{M_{fi,1,Ed}} = \frac{\mu_{fi,d} \cdot M_{fi,pl,Rd}}{M_{fi,1,Ed}} \tag{9}$$

b. Reordering eq. (6) gives the effective critical load as:

$$N_{fi,cr,eff} = \frac{N_{fi,Ed}}{1 - \frac{\beta}{k_{fi}}} \tag{10}$$

c. The effective flexural stiffness for second order analysis can be then computed from eq. (7):

$$\left(EI\right)_{fi,eff,II} = \frac{N_{fi,cr,eff} \cdot l_\theta^2}{\pi^2} \tag{11}$$

d. Finally, the correction factor for elevated temperatures can be obtained from eq. (8):

$$K_\theta = \frac{\left(EI\right)_{fi,eff,II}}{K_o\left[\varphi_{a,\theta} \cdot E_a(\theta_{a,eq}) I_a + \varphi_{s,\theta} \cdot E_s(\theta_{s,eq}) I_s + K_{e,II} \cdot \varphi_{c,\theta} \cdot E_c(\theta_{c,eq}) I_c\right]} \tag{12}$$

An extensive numerical parametric study, to be described in the next section, has been performed to obtain a consistent value for the correction factor $\left(K_\theta\right)$.

## 2.3 Results of parametric studies

### *2.3.1 Numerical model*

A three-dimensional numerical model was developed by means of the general purpose nonlinear finite element analysis package ABAQUS [18]. The model used a sequentially coupled thermal-stress analysis procedure, and was described in detail in a previous paper [16]. Geometric and material nonlinearities were accounted for in the numerical model. The model made use of the main heat transfer parameters recommended by EN 1991-1-2 [19]. The thermal resistance at the steel-concrete interface was taken into account through a constant value of 200 W/m$^2$K prescribed as a gap conductance. The initial geometric imperfection of the columns was considered by importing the first buckling mode shape of a hinged column, amplified by a factor of $L/1000$.

The model was meshed with three-dimensional eight-noded solid elements for both the steel tube and the concrete core, and two-noded solid elements for the reinforcing bars. The load was applied through a rigid body attached to the top end of the column, with all its nodes coupled to a reference point. This reference point was free to rotate and move along the longitudinal axis, but its displacement prevented in the other two directions. A second rigid plate was attached to the bottom end of the column, where all the displacements were prevented but rotational degrees of freedom were allowed. These rigid plates were meshed by using two-dimensional four-noded shell elements. Different loading points were defined into the loading plate at the top end of the column and the reaction plate at the bottom end, so that the loading conditions could be easily changed. Fig. 3 shows the details of the load application and finite element mesh for one column example with circular cross-section (A = 0.25$D$, B = 0.5$D$, C = 0.75$D$, D = 1$D$).

The thermal properties for concrete and steel at elevated temperatures were obtained from Clause 3.3 in EN 1994-1-2 [1] for steel-concrete composite structural elements. It should be pointed out that the upper limit of the concrete thermal conductivity was used, as recommended in Note 2, Clause 3.3.2(9). Also a 4% concrete moisture content was assumed in the model, as given in Clause 3.3.2(7) and the latent heat of water vaporisation was taken into account through a peak value in the specific heat capacity formulation between 100 and 200ºC, as per Clause 3.3.2(8).

For characterizing the mechanical behaviour of the materials, multi-axial models were used. For steel, an isotropic elastic-plastic model with the von Mises yield criterion was implemented. In turn, the Concrete Damage Plasticity (CDP) model was used for modelling the mechanical behaviour of concrete, which allows for a detailed definition of tensile and compressive behaviour of the material. Details of the input parameters used for the CDP model are provided in [16]. The constitutive models selected for representing the uniaxial behaviour of steel and concrete at elevated temperatures were those given by EN 1993-1-2 [20] and EN 1992-1-2 [21], respectively.

The numerical model is able to reproduce in a realistic way the fire performance of CFST columns with different cross-section shapes (CHS, SHS, EHS, RHS) and loading conditions (concentric and eccentric load), being fully validated with an extensive experimental database from the previous Project FRISCC [14, 16].

### *2.3.2 Analysed cases*

The previously described numerical model was used for conducting a comprehensive parametric study, which included all the practical ranges of the different parameters relevant to the fire design of CFST columns. The parameters studied were the outer diameter ($D$) or the larger and smaller outer dimensions ($H$ - $B$) in the case of rectangular and elliptical tubes

respectively, the wall thickness of the steel tube ($t$), the relative slenderness of the columns at room temperature ( $\overline{\lambda}$ ), the percentage of reinforcement ($\rho$), the concrete cover ($u_s$), the load level ($\mu$) and the relative eccentricity (*e/D, e/H or e/B*). The CFST column cases for the parametric studies were designed to meet the criteria of non-slender sections from EN1993-1-1 [22] and a steel contribution ratio between $0.2 \le \delta \le 0.9$. Moreover, to reflect practical situations of using CFST columns, the parametric study column cases lie within the range $L/D < 30$ and $t_{fi} \ge 30$ minutes. Fixed values were adopted for the following parameters: 4% moisture content, pinned-pinned boundary conditions, 355 MPa steel tube yield strength, 30 MPa concrete compressive strength and 500 MPa reinforcing bars yield strength.

For each geometry, 4 relative eccentricities about the minor axis ($e_y/B$) and 4 about the major axis ($e_z/H$) were used, being 0.25, 0.5, 0.75 and 1, generating for each column 8 different loading scenarios (see Fig. 4a). In the first instance, single curvature was considered ($r = e^{bottom}/e^{top} = 1$, Fig. 4b). In Section 2.5, non-uniform bending moment distributions (end moment ratios ($r = 0$ and $r = -1$)) will be evaluated.

Table 1 lists the combinations of parameters used in the parametric study. A total of 5046 analysis cases were obtained (1060 CHS, 1037 SHS, 660 RHS minor axis, 1304 RHS major axis, 348 EHS minor axis, 637 EHS major axis). The studied geometries are presented in Fig. 5.

All the columns were numerically simulated with the previously described numerical model, and the failure time was obtained for the load level applied in each case. From the results of the 5046 numerical simulations, an extensive numerical database of $N_{fi,Ed}$ - $t_{fi}$ relationships was obtained. It should be pointed out that, from the initial batch of analysis cases, some of them (less than 2% of the total number) had to be removed from the database due to excessive long fire resistance time beyond the scope of application of the simplified design method ($t_{fi}$ >

240 minutes) or exceedingly high relative slenderness at elevated temperature ( $\bar{\lambda}_\theta > 3$) which would not be practical.

### 2.4 Proposal for second order flexural stiffness at elevated temperatures

Applying the procedure described in Section 2.2 to the parametric study columns and after a statistical analysis of the results, the following equations for the correction coefficient for the second order flexural stiffness at elevated temperatures $\left(K_\theta\right)$ are proposed:

- for $t_{fi} \geq 60$ min:

$$K_\theta = 0.9 \tag{13}$$

- for $t_{fi} < 60$ min:

$$K_\theta = 0.5 + 160\rho_s^2 \tag{14}$$

where $\rho_s$ is the percentage of reinforcement.

Fig. 6 compares the numerical simulation results with the calculation results using the proposed simplified method and the proposed correction coefficient $K_\theta$.

Table 2 gives the average of ratios of the numerical simulation failure load of the CFST column to the predicted failure load by using the simplified design method at the numerically obtained failure time. As can be seen, the mean value lies on the safe side (over one) for all the column geometries studied.

It should be noted that the proposed method inherits the conservativeness existing in cold design [23], made more evident at elevated temperatures due to the additional reduction factors.

### 2.5 Variable bending moment along column

The study for constant bending moment diagram (i.e. end moment ratio $r = e^{bottom}/e^{top} = 1$) has established the simplified calculation method. However, in practical applications, non-constant bending moment diagrams are often found. A further parametric study has been carried out for columns with variable bending moments to check that the same method is also applicable, based on a subset of cases from the parametric studies for constant bending moment presented in Section 2.3.2. Table 3 lists a total 72 column cases which comprise of the following: 139.7×12.5 mm (small $D/t$) and 508×10 mm (large $D/t$) (with relative slenderness of 0.3 and 0.7, respectively); three load ratios of 15, 30 and 60%; four relative eccentricities of $e/D$ = 0.25, 0.5, 0.75 and 1; and two end moment ratios of $r$ = -1 and $r$ = 0, see Fig. 7. For the larger section, a 5% reinforcement was included. The material strengths were fixed to be $f_y$ = 355 MPa, $f_s$ = 500 MPa and $f_c$ = 30 MPa and the boundary conditions were in all cases pinned-pinned.

Fig. 8 compares the numerical simulation and simplified calculation method results. It can be observed that most of the cases lie on the safe side, with an average ratio of numerical simulation failure load to calculation result of 1.45 and a standard deviation of 0.54. The scatter is higher than for constant bending moment distribution, but is considered acceptable given the complexity of the loading situation and simplicity of the proposed design calculation method.

### 2.6 Comparison with experiments

To further demonstrate accuracy of the proposed simplified design method, its calculation results are compared against the results of a number of fire tests with eccentric loading. The fire test data were from France [24, 25], Germany [26], Spain [27], Canada [28], as well as from the experimental campaign of the European Project FRISCC [29, 30], which included large eccentricities and different cross-sectional geometries (including RHS and EHS). These give a

total of 46 fire tests with eccentric loading. Of these, only 33 were selected so that they are within the scope of application of the simplified design method according to $L/D < 30$ and $t_{fi} \geq$ 30 minutes.

Fig. 9 compares results of the fire tests and calculations using the simplified design method. Again, the simplified design method gives results on the safe side in most cases.

For a new fire design method to be acceptable, the CEN/TC250 Horizontal Group Fire [31] has defined the following acceptance criteria: 1) the calculation result shall not be on the unsafe side by more than 15% of the reference result; 2) the number of individual calculation results on the unsafe side shall not exceed a maximum of 20%; and 3) the mean value of ratios of the reference result to the calculation result shall be on the safe side (>1).

Table 4 compares the statistics for the simplified design method against the above acceptance criteria. The criteria are met in all three cases. Therefore, the proposed simplified design method is considered to be acceptable for fire resistance design of CFST columns under eccentric loading.

## 3 SUMMARY OF THE PROPOSED SIMPLIFIED DESIGN METHOD

For ease of use, the complete simplified design method, for the case of calculating the load carrying capacity of a CFST column at a given fire resistance time, is described below:

1. Calculate the equivalent temperatures of the cross-section components ( $\theta_{a,eq}, \theta_{c,eq}, \theta_{s,eq}$ ) using equations (1), (2) and (3). The reduction factors for strength and modulus of elasticity of the materials can be obtained using Tables 3.2 and 3.3 in EN1994-1-2 [1].
2. Calculate the cross-section plastic resistance and second order effective flexural stiffness values by summing up the contribution of each component:

Cross-section plastic resistance:

$$N_{\mathrm{fi,pl,Rd}} = A_a f_y(\theta_{a,eq}) + A_c f_c(\theta_{\mathrm{c},eq}) + A_s f_s(\theta_{\mathrm{s},eq}) \tag{15}$$

Second order effective flexural stiffness:

$$(EI)_{\mathrm{fi,eff,II}} = K_\theta \cdot K_o \cdot \left[ \varphi_{a,\theta} \cdot E_a(\theta_{a,eq}) I_a + \varphi_{\mathrm{s},\theta} \cdot E_s(\theta_{\mathrm{s},eq}) I_s + K_{e,II} \cdot \varphi_{\mathrm{c},\theta} \cdot E_c(\theta_{\mathrm{c},eq}) I_c \right] \tag{16}$$

where the correction factor $K_\theta$ for elevated temperatures are from equation (13) or (14).

The critical buckling load at elevated temperatures can be calculated as follows:

$$N_{\mathrm{fi,cr,eff}} = \frac{\pi^2 (EI)_{\mathrm{fi,eff,II}}}{l_\theta^2} \tag{17}$$

3. Quantify the cross-sectional axial force-bending moment (N-M) plastic interaction diagram, using the same method as for cold design but elevated temperature design strengths of materials.

4. Find the column load carrying capacity. The applied load is increased until the second order bending moment – compressive force ($M_{\mathrm{fi,Ed}}$ - $N_{\mathrm{fi,Ed}}$) loading curve intersects with the cross-sectional M-N interaction curve at elevated temperatures.

For a given axial load value $N_{\mathrm{fi,Ed}}$, the second order bending moment can be computed, in the same way as for cold design, by magnifying the contributions of load eccentricity and initial imperfection:

$$M_{\mathrm{fi,Ed}} = N_{\mathrm{fi,Ed}} \cdot e \cdot k_{fi} + N_{\mathrm{fi,Ed}} \cdot e_{imp} \cdot k_{fi,imp} \tag{18}$$

The same member imperfection ($e_{imp}$) as in Table 6.5 of EN1994-1-1 [17], as a function of the percentage of reinforcement, can be used for fire design. The $k_{fi}$ factors are calculated in the same way as in cold design, as follows:

$$k_{fi} = \frac{\beta}{1 - \frac{N_{\text{fi,Ed}}}{N_{\text{fi,cr,eff}}}} \tag{19}$$

where $\beta$ is an equivalent moment factor given in Table 6.4 of EN1994-1-1 [17], depending on the end moment ratio and moment distribution. For member imperfection, which gives a parabolic distribution of moments, $\beta$ = 1; for moments from eccentricity with a linear distribution of bending moments,

$$\beta = 0.66 + 0.44r \quad \text{but } \beta \geq 0.44 \tag{20}$$

As $k_{fi}$ is dependent on the value of the axial load $N_{\text{fi,Ed}}$, an iterative process is necessary.

The column failure load is the value that fulfils the following condition:

$$\frac{M_{\text{fi,Ed}}}{M_{\text{fi,pl,N,Rd}}} = \frac{M_{\text{fi,Ed}}}{\mu_{\text{fi,d}} M_{\text{fi,pl,Rd}}} \leq \alpha_{\text{M}} \tag{21}$$

For steel grades between S235 and S355 inclusive, the coefficient $\alpha_{\text{M}}$ should be taken as 0.9, while for steel grades S420 and S460, a value of 0.8 should be used, as in cold design.

Should it be necessary to obtain the column fire resistance time at a given applied load, the iterative process should operate in the time domain.

### 3.1 Applicability limits of the proposed method

The proposed simplified design method should only be applied for CFST columns in the following conditions:

- Section factor ($A_m/V$), cross-sectional slenderness ($D/t$ or $B/t$), member slenderness ($l_\theta/D$ or $l_\theta/B$)and aspect ratio ($H/B$):

| **CHS** | **SHS** | **EHS** | **RHS** |
|---|---|---|---|
| $5 \leq A_m/V \leq 30$ | $5 \leq A_m/V \leq 35$ | $10 \leq A_m/V \leq 30$ | $10 \leq A_m/V \leq 45$ |

| | | | |
|---|---|---|---|
| $10 \le D/t \le 60$ | $5 \le B/t \le 40$ | $5 \le B/t \le 20$ | $5 \le B/t \le 20$ |
| $5 \le l_\theta / D \le 30$ | $5 \le l_\theta / B \le 30$ | $5 \le l_\theta / B \le 30$ | $5 \le l_\theta / B \le 30$ |
| | | $H/B = 2$ | $H/B = \{1.5, 2, 3\}$ |

- The percentage of reinforcement shall be lower than 5 %.
- The relative load eccentricity $e/D$, $e/\mathrm{B}$ or $e/\mathrm{H}$ shall not exceed 1.
- Fire exposure times between 30 and 240 minutes.
- Unprotected columns in braced frames.
- Eccentric loading about one axis only.
- The maximum relative slenderness at elevated temperature is $\overline{\lambda}_o = 3$.

## 4 WORKED EXAMPLE

A worked example is provided to illustrate application of the proposed simplified calculation method. Fig. 10 shows the cross-sectional dimensions of a circular column.

a. Input data

- Cross-section dimensions: $D \times t = 273 \times 5$ mm
- Standard fire period: R30 ($t_{fi} = 30$ min)
- Column length: $L$ = 4 m (pinned at both ends)
- Reinforcement: $10\phi 12$ mm $\left(\rho_s = 2,08\%\right)$
- Concrete cover (rebar axis distance): $u_s = 35$ mm
- Load eccentricity: $e$ = 136.5 mm $\left(e/D = 0,5\right)$
- Structural steel yield strength: $f_y = 355$ MPa
- Concrete compressive strength: $f_c = 30$ MPa
- Reinforcing steel yield strength: $f_s = 500$ MPa

b. Preliminary calculations

Section factor: $$A_m / V = \frac{\pi D}{\frac{\pi}{4} D^2} = \frac{4}{D} = \frac{4}{273} \times 1000 = 14,652 \text{ m}^{-1}$$

Areas and moments of inertia:

- Steel tube: $A_a = 4209,7 \text{ mm}^2$; $I_a = 3,7808 \cdot 10^7 \text{ mm}^4$
- Concrete core: $A_c = 53194 \text{ mm}^2$; $I_c = 22,958 \cdot 10^7 \text{ mm}^4$
- Reinforcing bars: $A_s = 1131 \text{ mm}^2$; $I_s = 5,2761 \cdot 10^6 \text{ mm}^4$

c. Equivalent temperatures and reduced material properties

Steel tube:

$$\theta_{a,eq} = -824,67 - 5,58 \cdot 30 + 0,007 \cdot 30^2 - 0,01 \cdot 30 \cdot 14,652 + 645,08 \cdot 30^{0,269} \cdot 14,652^{0,017} = 696 \text{ ºC}$$

$$k_y\left(\theta_{a,eq}\right) = 0,2396; f_y\left(\theta_{a,eq}\right) = 85,06 \text{ MPa}$$

$$k_{\mathrm{E}}\left(\theta_{a,eq}\right) = 0,1372; E_a\left(\theta_{a,eq}\right) = 28812 \text{ MPa}$$

Concrete core:

$$\theta_{c,eq} = 81,8 - 5,05 \cdot 30 + 0,003 \cdot 30^2 - 15,07 \cdot 14,652 + 0,3 \cdot 14,652^2 - 0,88 \cdot 30 \cdot 14,652 + \\ + 7,43 \cdot 30^{0,842} \cdot 14,652^{0,714} = 284 \text{ ºC}$$

$$k_{\mathrm{c}}\left(\theta_{\mathrm{c},eq}\right) = 0,866; f_c\left(\theta_{\mathrm{c},eq}\right) = 25,98 \text{ MPa}$$

$$\varepsilon_{\mathrm{cu}}\left(\theta_{\mathrm{c},eq}\right) = 0,0068; E_c\left(\theta_{\mathrm{c},eq}\right) = \frac{f_c\left(\theta_{\mathrm{c},eq}\right)}{\varepsilon_{cu}\left(\theta_{\mathrm{c},eq}\right)} = 3820,6 \text{ MPa}$$

Reinforcing bars $\left(u_s = 35 \text{ mm}\right)$:

$$\theta_{s,eq} = \beta_3 \cdot \left(30/35^2\right)^3 + \beta_2 \cdot \left(30/35^2\right)^2 + \beta_1 \cdot \left(30/35^2\right) + \beta_0 = \\ = 0 \cdot \left(30/35^2\right)^3 - 12732 \cdot \left(30/35^2\right)^2 + 6518 \cdot \left(30/35^2\right) + 91,208 = 243 \text{ ºC}$$

$$k_y\left(\theta_{\mathrm{s},eq}\right) = 1,0; \; f_s\left(\theta_{\mathrm{s},eq}\right) = 500 \text{ MPa}$$

$$k_{\mathrm{E}}\left(\theta_{\mathrm{s},eq}\right)=0,8052;\ E_s\left(\theta_{\mathrm{s},eq}\right)=169092\ \mathrm{MPa}$$

d. Flexural stiffness reduction coefficients and stiffness correction factor:

Concrete core: $\varphi_{\mathrm{c},\theta}=1,2$ (for secant modulus)

Steel tube: $\varphi_{a,\theta}=0,75-0,023\cdot\left(A_m/V\right)=0,75-0,023\cdot 14,652=0,413$

Reinforcement: $\varphi_{\mathrm{s},\theta}=0,8-0,002\cdot t_{fi}=0,8-0,002\cdot 30=0,74$

Additionally, the stiffness correction factor at elevated temperatures for second order effects is $K_\theta=0,5+160\rho_s^2=0,5+160\cdot 0,0208^2=0,5693$, from Section 2.4.

e. Cross-section plastic resistance and effective flexural stiffness

Cross-section plastic resistance:

$$N_{\mathrm{fi,pl,Rd}}=A_a f_y(\theta_{a,eq})+A_c f_c(\theta_{\mathrm{c},eq})+A_s f_s(\theta_{\mathrm{s},eq})=2305,6\ \mathrm{kN}$$

Effective second order flexural stiffness:

$$(EI)_{\mathrm{fi,eff,II}}=K_\theta\cdot K_o\cdot\left[\varphi_{a,\theta}\cdot E_a(\theta_{a,eq})I_a+\varphi_{\mathrm{s},\theta}\cdot E_s(\theta_{\mathrm{s},eq})I_s+K_{e,II}\cdot\varphi_{\mathrm{c},\theta}\cdot E_c(\theta_{\mathrm{c},eq})I_c\right]=$$
$$=0,5693\cdot 0,9\cdot\left[\varphi_{a,\theta}\cdot E_a(\theta_{a,eq})I_a+\varphi_{\mathrm{s},\theta}\cdot E_s(\theta_{\mathrm{s},eq})I_s+0.5\cdot\varphi_{\mathrm{c},\theta}\cdot E_c(\theta_{\mathrm{c},eq})I_c\right]=8,4011\cdot 10^{11}\ \mathrm{N\cdot mm^2}$$

f. Construction of the M-N interaction curve at elevated temperatures

Plastic section moduli (according to EN 10210-2 [32]):

Steel tube:

$$W_{pa}=\frac{D^3-\left(D-2t\right)^3}{6}=3,5916\cdot 10^5\ \mathrm{mm^3}$$

Reinforcing bars:

$$W_{ps}=\sum_{i=1}^{n}A_{si}\cdot e_i=7,0636\cdot 10^4\ \mathrm{mm^3}$$

where $e_i$ is the distance of the i$^{\mathrm{th}}$ reinforcing bar to the centre line of the transverse cross-section.

Concrete core:

$$W_{pc} = \frac{(D-2t)^3}{6} - W_{ps} = 2{,}9613{\cdot}10^6 \text{ mm}^3$$

The distance $h_n$ from the centre-line of the composite cross-section to the plastic neutral axis in the situation of pure bending can be obtained as follows:

$$h_n = \frac{A_c \cdot f_c - A_{sn} \cdot (2f_s - f_c)}{2D \cdot f_c + 4t \cdot (2f_y - f_c)} = 55{,}153 \text{ mm}$$

In this example, it is initially considered that 4 reinforcing bars lie within the region of depth $2h_n$ and $A_{sn} = 4\phi12 = 452.39$ mm$^2$. The resulting plastic neutral axis distance ($h_n = 55.153$ mm) confirms the hypothesis, as the 4 rebars close to the centre line of the section are located at a distance of 29.7 mm, whereas the second group of 4 rebars are at a distance of 78 mm, and therefore lie outside of the region of a depth $2h_n$ as shown in Fig. 10.

Plastic section moduli of the corresponding components within the region $2h_n$:

Steel tube:

$$W_{pan} = 2t \cdot h_n^2 = 3{,}0419{\cdot}10^4 \text{ mm}^3$$

Reinforcing bars:

$$W_{psn} = 1{,}349{\cdot}10^4 \text{ mm}^3$$

where $W_{psn}$ corresponds to the plastic moduli of the 4 rebars which lie within the region of depth $2h_n$.

Concrete core:

$$W_{pcn} = (D-2t) \cdot h_n^2 - W_{psn} = 7{,}8652{\cdot}10^5 \text{ mm}^3$$

Now, the relevant points of the M-N interaction curve can be obtained (see Fig. 11):

- Point A:

$$N_{A,Rd} = N_{fi,pl,Rd} = 2305{,}6 \text{ kN}; \; M_{A,Rd} = 0 \text{ kN}{\cdot}\text{m}$$

- Point B:

$$N_{\mathrm{B},Rd} = 0 \text{ kN};\ M_{\mathrm{B},Rd} = M_{fi,pl,Rd} = 84,76 \text{ kN·m}$$

where

$$M_{fi,pl,Rd} = (W_{pa} - W_{pan})\cdot f_y\left(\theta_{a,eq}\right) + \frac{1}{2}(W_{pc} - W_{pcn})\cdot f_c\left(\theta_{\mathrm{c},eq}\right) + (W_{ps} - W_{psn})\cdot f_s\left(\theta_{\mathrm{s},eq}\right) = 84,76 \text{ kN·m}$$

- Point C:

$$N_{\mathrm{C},Rd} = A_c f_c\left(\theta_{c,eq}\right) = 1382 \text{ kN};\ M_{\mathrm{C},Rd} = M_{fi,pl,Rd} = 84,76 \text{ kN·m}$$

- Point D:

$$N_{\mathrm{D},Rd} = A_c f_c\left(\theta_{c,eq}\right)/2 = 691 \text{ kN};\ M_{\mathrm{D},Rd} = M_{fi,\max,Rd} = 104,34 \text{ kN·m}$$

where $M_{fi,\max,Rd} = W_{pa}\cdot f_y\left(\theta_{a,eq}\right) + \frac{1}{2}W_{pc}\cdot f_c\left(\theta_{\mathrm{c},eq}\right) + W_{ps}\cdot f_s\left(\theta_{\mathrm{s},eq}\right) = 104,34 \text{ kN·m}$

The design M-N interaction diagram is reduced by multiplying the bending moment of the above M-N diagram by 0.9, according to equation (21). These two curves are shown in Fig. 11.

g. Calculation of the second order bending moment

In this case, it is assumed that the bending moment from eccentricity is uniform along the column (i.e. same eccentricity at both column ends), while the moment from the member imperfection is parabolic with the maximum value at the mid-height. Thus, the second order bending moment comprises of two components:

$$M_{fi,Ed} = \left(k_{fi}\cdot e + k_{fi,imp}\cdot e_{imp}\right)N_{fi,Ed}$$

The member imperfection is assumed to be $e_{imp} = L/300$ following EN 1994-1-1 [17] Table 6.5 for $\rho_s \le 3\%$.

The amplification factor for each component of the bending moment can be obtained as follows:

- For the moment from eccentricity: $r = 1;\ \beta = 0,66 + 0,44 \cdot 1 = 1,1;\ k_{fi} = \dfrac{1,1}{1 - \dfrac{N_{fi,Ed}}{N_{fi,cr,eff}}}$

- For the moment from imperfection: $\beta = 1;\ k_{fi,imp} = \dfrac{1}{1 - \dfrac{N_{fi,Ed}}{N_{fi,cr,eff}}}$

The critical buckling load for second order effects is obtained as follows:

$$N_{fi,cr,eff} = \frac{\pi^2 \left(EI\right)_{fi,eff,II}}{l_\theta^2} = 518,22 \text{ kN}$$

Note that the effective length of the column is taken as the column length, $l_\theta = 4$ m.

After these calculations, the fire design of the column may be performed for one of the following two checks:

**I. Check A: to find the ultimate load (iterative solution)**

In order to obtain the ultimate load of the column in the fire situation, the applied load ($N_{fi,Ed}$) can be increased progressively up to the intersection point with the M-N interaction diagram at the elevated temperatures corresponding to the design fire resistance time.

The red dashed line in Fig. 11 shows the applied axial load – second order bending moment ($N_{fi,Ed}$-$M_{fi,Ed}$) interaction curve. This curve intercepts the reduced M-N diagram of the CFST composite cross-section at a load of **256.17 kN** and this is the column failure load in fire.

**II. Check B: Verification of the column for a given design load (direct solution)**

In some situations, the design load in fire is given and the design calculation is to check whether this load exceeds the resistance of the column.

Assume the applied load in the fire situation is $N_{fi,Ed}$ = 200 kN.

At the point of intersection between the horizontal line of $N_{fi,Ed}$ = 200 kN (the grey dashed line in Fig. 11) and M-N diagram:

$$M_{fi,pl,N,Rd} = \mu_{fi,d} \cdot M_{fi,pl,Rd} = 90,45 \text{ kN·m}$$

The amplification factors are:

$$k_{fi} = \frac{1,1}{1-\frac{200}{518,22}} = 1,7913;\ k_{fi,imp} = \frac{1}{1-\frac{200}{518,22}} = 1,6285$$

The second order bending moment is calculated as:

$$M_{fi,Ed} = \left(k_{fi} \cdot e + k_{fi,imp} \cdot e_{imp}\right) N_{fi,Ed} = \left(1,7913 \cdot 0,1365 + 1,6285 \cdot \frac{4}{300}\right) \cdot 200 = 53,25 \text{ kN} \cdot \text{m}$$

At the design axial load:

$$\frac{M_{fi,Ed}}{M_{fi,pl,N,Rd}} = \frac{53,25}{90,45} = 0,59 < \alpha_M = 0,9 \rightarrow \text{SAFE}$$

The result shows that the applied load $N_{fi,Ed}$ of 200 kN is allowable for this column.

In fact, (53.25 kN.m, 200 kN) is one point on the $M_{fi,Ed}$-$N_{fi,Ed}$ curve Check A.

## 5 SUMMARY AND CONCLUSIONS

This paper has presented the development of a simplified fire design method for eccentrically loaded CFST columns, valid for different cross-section shapes, slenderness and all types of bending conditions (constant and variable bending moment).

This simplified design method calculates equivalent uniform temperatures for the three different components (steel tube, concrete, reinforcement) of a CFST column, thus converting the fire design into cold design. The focus of this paper was to check the validity of the proposed simplified calculation method for eccentrically loaded CFST columns and to identify any additional modification to the cross-section flexural stiffness for second order analysis. This was achieved by comparing the results of an extensive set of parametric study, using a previously validated numerical model, against the results of the simplified design method.

Using the results of 33 fire tests on CFST columns under eccentric loading as reference values, it has been shown that the proposed simplified method meets the acceptance criteria defined by the CEN/TC250 Horizontal Group Fire. Therefore, it can be accepted for practical applications. Finally, a worked example has been provided to illustrate application of the proposed simplified method for the fire design of eccentrically loaded CFST columns.

## ACKNOWLEDGEMENTS

The authors would like to express their sincere gratitude to the “Conselleria d’Educació, Investigació, Cultura i Esport” of the Valencian Community (Spain) for the help provided through project GV/2017/026. The authors also acknowledge the funding received from the European Committee for Standardization (CEN) for the Project Team SC4.T4 of CEN/TC250, through the grant agreement CEN/2014-02 Mandate M/515 Phase 1.

## REFERENCES

[1] CEN. EN 1994-1-2, Eurocode 4: Design of composite steel and concrete structures. Part 1-2: General rules - Structural fire design. Brussels, Belgium: Comité Européen de Normalisation; 2005.

[2] Romero ML, Moliner V, Espinos A, Ibanez C, Hospitaler A. Fire behavior of axially loaded slender high strength concrete-filled tubular columns. J Constr Steel Res. 2011;67:1953-65.

[3] Leskela MV. Inconsistencies in the fire design rules of composite columns to EN 1994-1-2. Steel concrete composite and hybrid structures. Leeds, England;2009. p. 489-94.

[4] CEN. CEN/TC 250/SC4 - N358. Resolutions agreed at the SC4 Vienna meeting. 2011.

[5] Aribert JM, Renaud C, Zhao B. Simplified fire design for composite hollow-section columns. Proc Inst Civil Eng-Struct Build. 2008;161:325-36.

[6] Renaud C, Joyeux D, Kruppa J. Improvement and extension of the simple calculation method for fire resistance of unprotected concrete filled hollow columns. In: 15Q-12/03 Crp, editor. Saint-Rémy-lès-Chevreuse, France: Centre Technique Industriel de la Contruction Métallique (CTICM); 2004.

[7] Building Department of Environmental Ministry of Finland. National selections for Finland regarding standard SFS-EN 1994-1-2, Design of composite steel and concrete structures - Part 1-2: General rules - Structural fire design. Fire design method replacing the simple calculation method of informative Annex H of SFS-EN 1994-1-2 for concrete filled hollow sections (draft version). 2016.

[8] Wang YC. Design guide for concrete filled hot finished structural hollow sections (SHS) columns. TATA Steel. 2014.

[9] Espinos A, Romero ML, Hospitaler A. Simple calculation model for evaluating the fire resistance of unreinforced concrete filled tubular columns. Eng Struct. 2012;42:231-44.

[10] Espinos A, Romero ML, Hospitaler A. Fire design method for bar-reinforced circular and elliptical concrete filled tubular columns. Eng Struct. 2013;56:384-95.

[11] Kodur VKR, Mackinnon DH. Design of concrete-filled hollow structural steel columns for fire endurance. Engineering Journal. 2000;37:13-24.

[12] Han LH, Zhao XL, Yang YF, Feng JB. Experimental study and calculation of fire resistance of concrete-filled hollow steel columns. Journal of Structural Engineering. 2003;129:346-56.

[13] ANUHT. Fire resistance design of non-insulated CFT columns - guidelines, technical explanations and deign examples. 2004.

[14] Fire resistance of innovative and slender concrete filled tubular composite columns (FRISCC). Final Report. Catalogue number KI-NA-28082-EN-N, RFCS Publications. European Commission. Brussels: Research Fund for Coal and Steel; 2016.

[15] Wang YC, Orton AH. Fire resistant design of concrete filled tubular steel columns. The Structural Engineer. 2008;7:40-5.

[16] Albero V, Espinos A, Romero ML, Hospitaler A, Bihina G, Renaud C. Proposal of a new method in EN1994-1-2 for the fire design of concrete-filled steel tubular columns. Eng Struct. 2016;128:237-55.

[17] CEN. EN 1994-1-1, Eurocode 4: Design of composite steel and concrete structures. Part 1-1: General rules and rules for buildings. Brussels, Belgium: Comité Européen de Normalisation; 2004.

[18] ABAQUS. Abaqus/Standard Version 6.14 User's Manual: Volumes I-III. Pawtucket, Rhode Island: Hibbit, Karlsson & Sorensen, Inc. 2014.

[19] CEN. EN 1991-1-2, Eurocode 1: Actions on structures. Part 1-2. General actions - actions on structures exposed to fire. Brussels, Belgium: Comité Européen de Normalisation; 2002.

[20] CEN. EN 1993-1-2, Eurocode 3: Design steel structures. Part 1-2: General rules - Structural fire design. Brussels, Belgium: Comité Européen de Normalisation; 2005.

[21] CEN. EN 1992-1-2, Eurocode 2: Design of concrete structures. Part 1-2: General rules - Structural fire design. Brussels, Belgium: Comité Européen de Normalisation; 2004.

[22] CEN. EN 1993-1-1, Eurocode 3: Design steel structures. Part 1-1: General rules and rules for buildings. Brussels, Belgium: Comité Européen de Normalisation; 2005.

[23] Espinós A, Albero, V., Romero, M.L., Mund, M., Kleiboemer, I., Meyer, P., Schaumann, P. Numerical investigation on slender concrete-filled steel tubular columns subjected to biaxial bending. 12th International Conference on Advances in Steel-Concrete Composite Structures (ASCCS 2018). Valencia: Universitat Politècnica de València; 2018.

[24] CIDECT. Stabilité au feu des profils creux en acier de construction. Final report no. 76/36 – 15 A. Cometube; 1976.

[25] Renaud C. Unprotected concrete filled columns fire tests – Verification of 15 Q. CIDECT Research Project 15 R. Final report. 2004.

[26] Deutschen Stahlbau verband, Stahlbau Handbuck, Band 1, Zweite Nuebearbeitete Auflage. Kolr, Satlbau-Verlags-GmbH. 1982.

[27] Moliner V, Espinos A, Romero ML, Hospitaler A. Fire behavior of eccentrically loaded slender high strength concrete-filled tubular columns. Journal of Constructional Steel Research. 2013;83:137-46.

[28] Chabot M LT. Experimental studies on the fire resistance of hollow steel columns filled with plain concrete, National Research Council Canada, Institute for Research in Construction. Internal report 611. 1992.

[29] Espinos A, Romero ML, Serra E, Hospitaler A. Experimental investigation on the fire behaviour of rectangular and elliptical slender concrete-filled tubular columns. Thin-Walled Structures. 2015;93:137-48.

[30] Espinos A, Romero ML, Serra E, Hospitaler A. Circular and square slender concrete-filled tubular columns under large eccentricities and fire. J Constr Steel Res. 2015;110:90-100.

[31] Fire C-T-HG. EUROCODES - FIRE PARTS. Proposal for a Methodology to check the Accuracy of Assessment Methods. France: CTICM; 2014.

[32] CEN. EN 10210-2. Hot finished structural hollow sections of non-alloy and fine grain steels - Part 2: Tolerances, dimensions and sectional properties. 2006.

Albero V, Espinós A, Romero ML, Wang YC, Renaud C, Schaumann P, Nigro E. Interaction diagram based method for fire resistance design of eccentrically loaded concrete-filled steel tubular columns. Thin-Walled Structures 2018; 130:641-651. doi: https://doi.org/10.1016/j.tws.2018.06.017

**FIGURES**

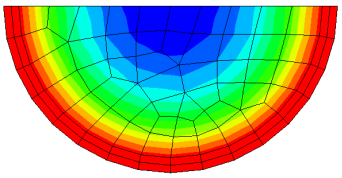

Realistic temperature field

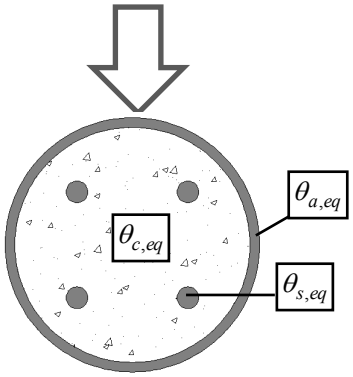


Equivalent temperature field

Fig. 1 Simplification of the temperature field.

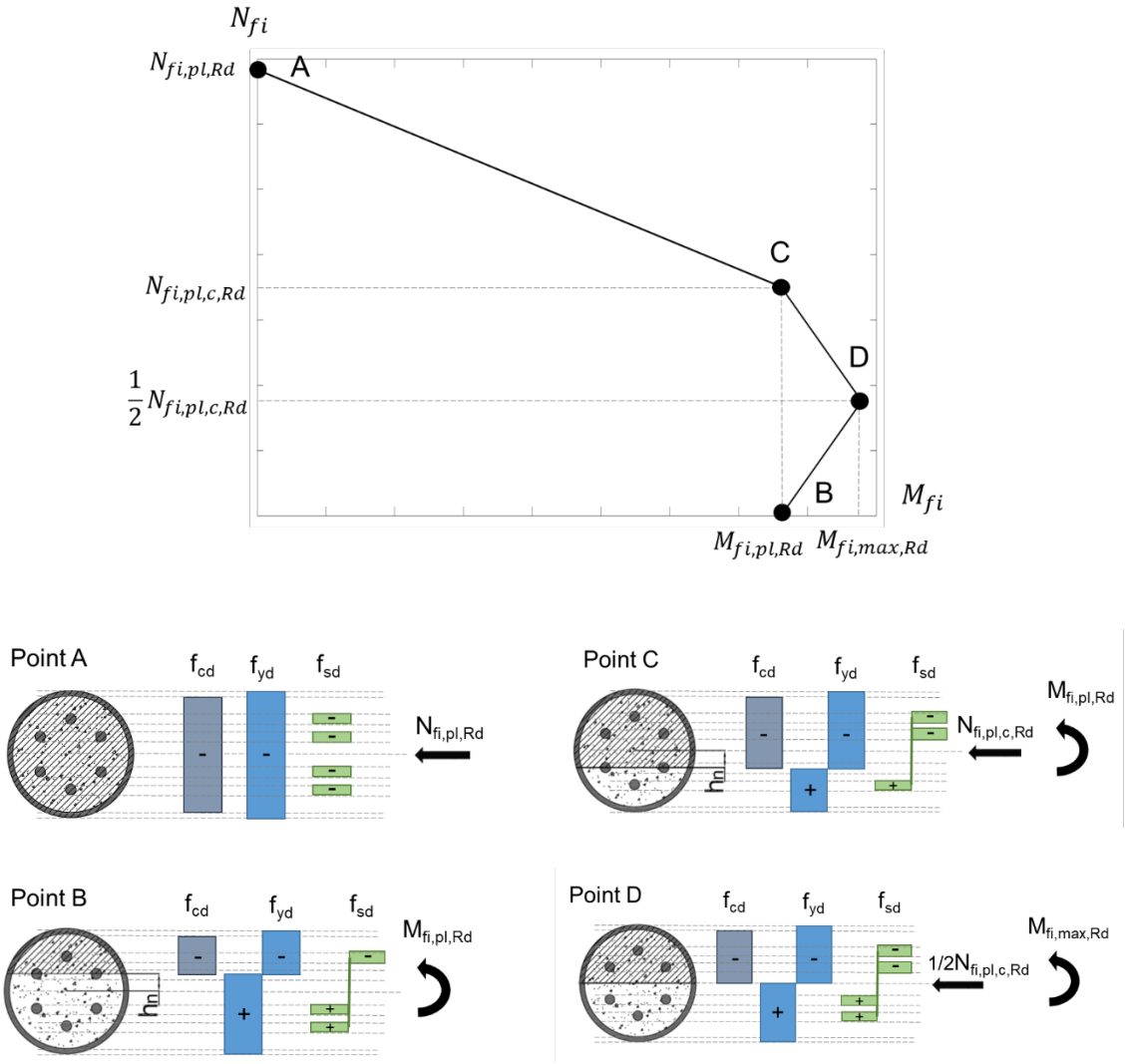


Fig. 2 M-N Interaction diagram at elevated temperature.

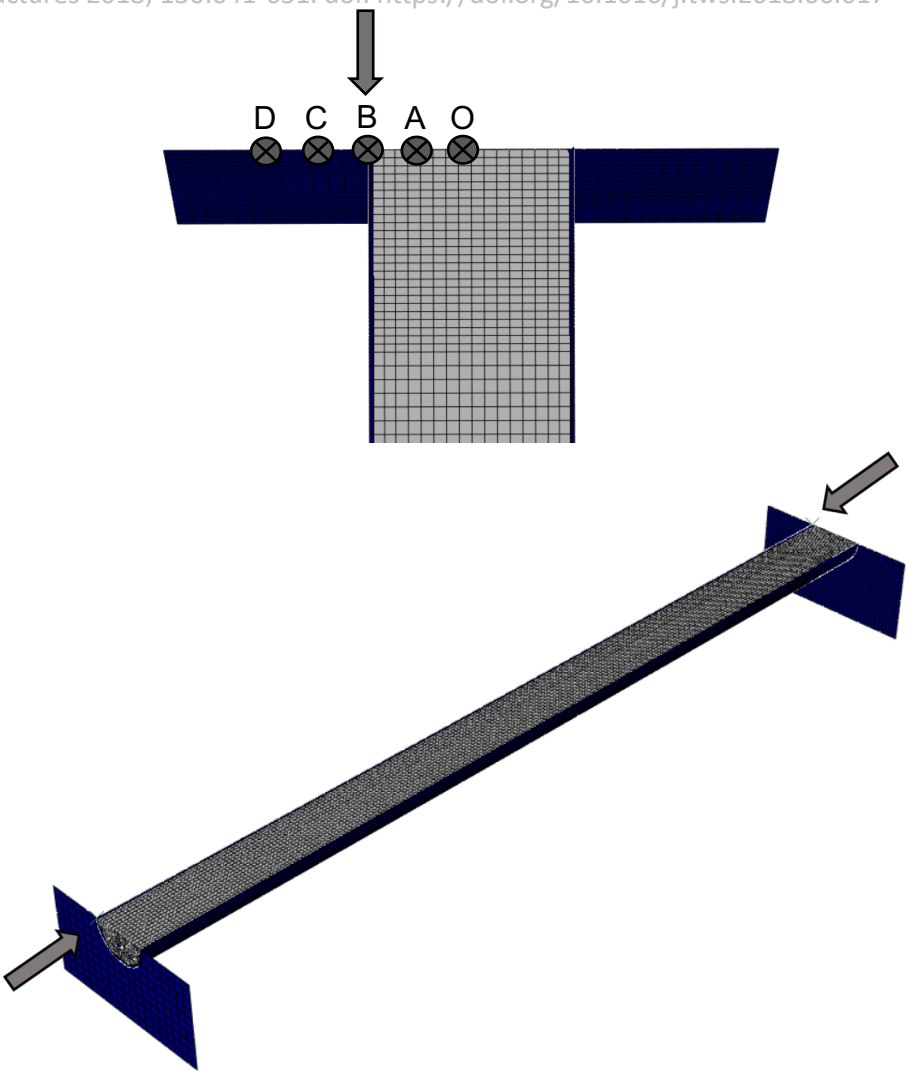


Fig. 3 Details of the finite element mesh and points of load application.

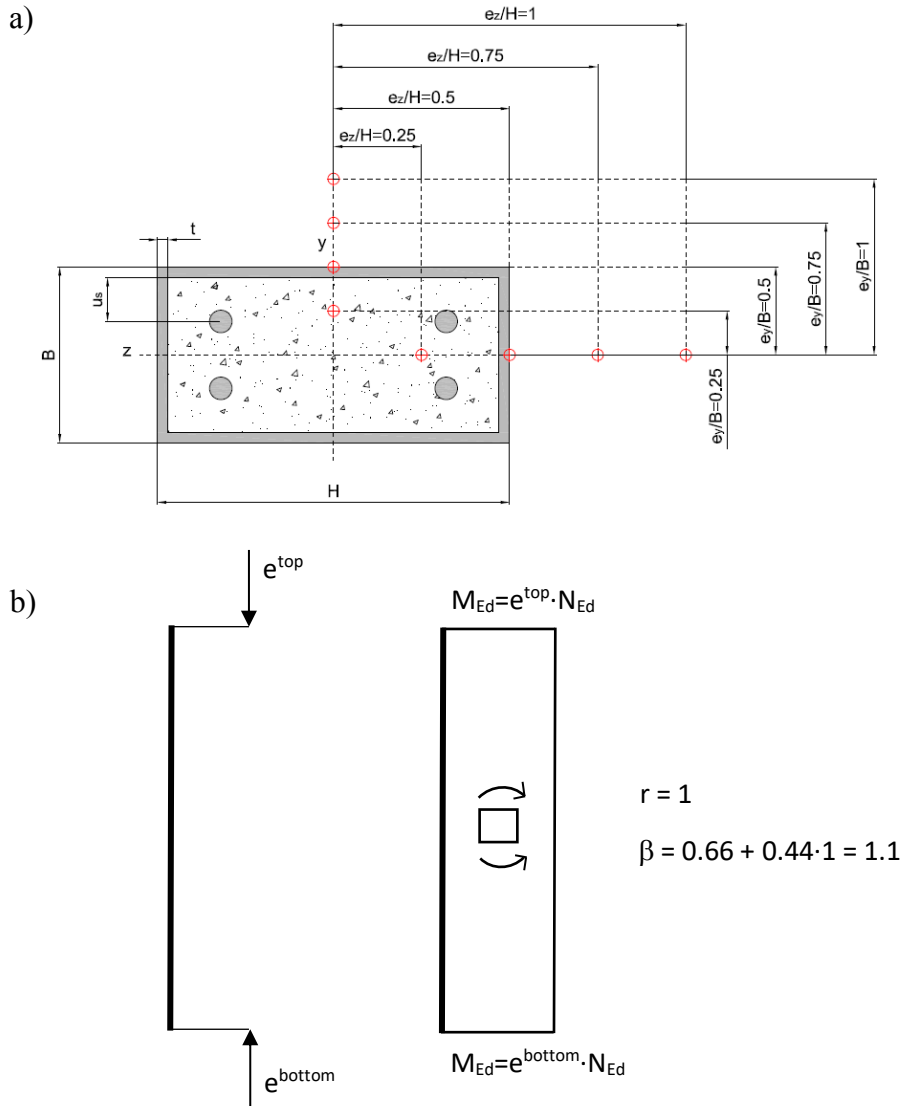


Fig. 4 Points of load application (a) and end moment distribution (b) in the parametric studies.

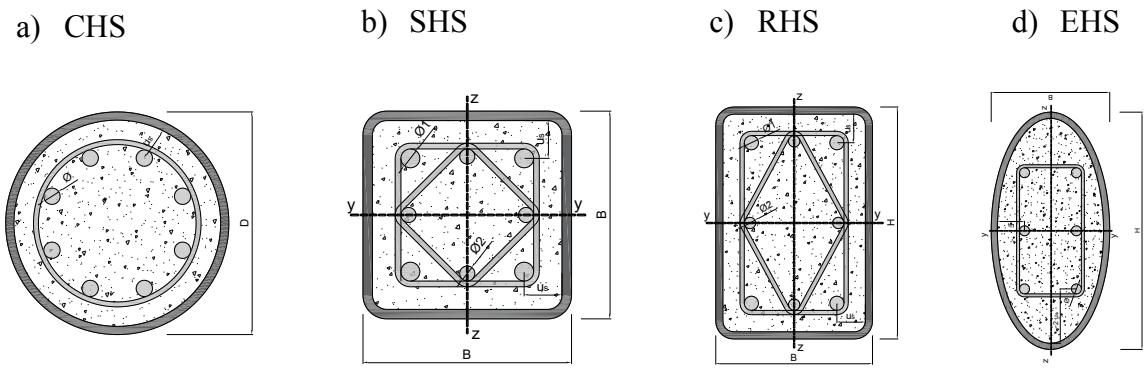


Fig. 5 Sections used in the parametric studies.

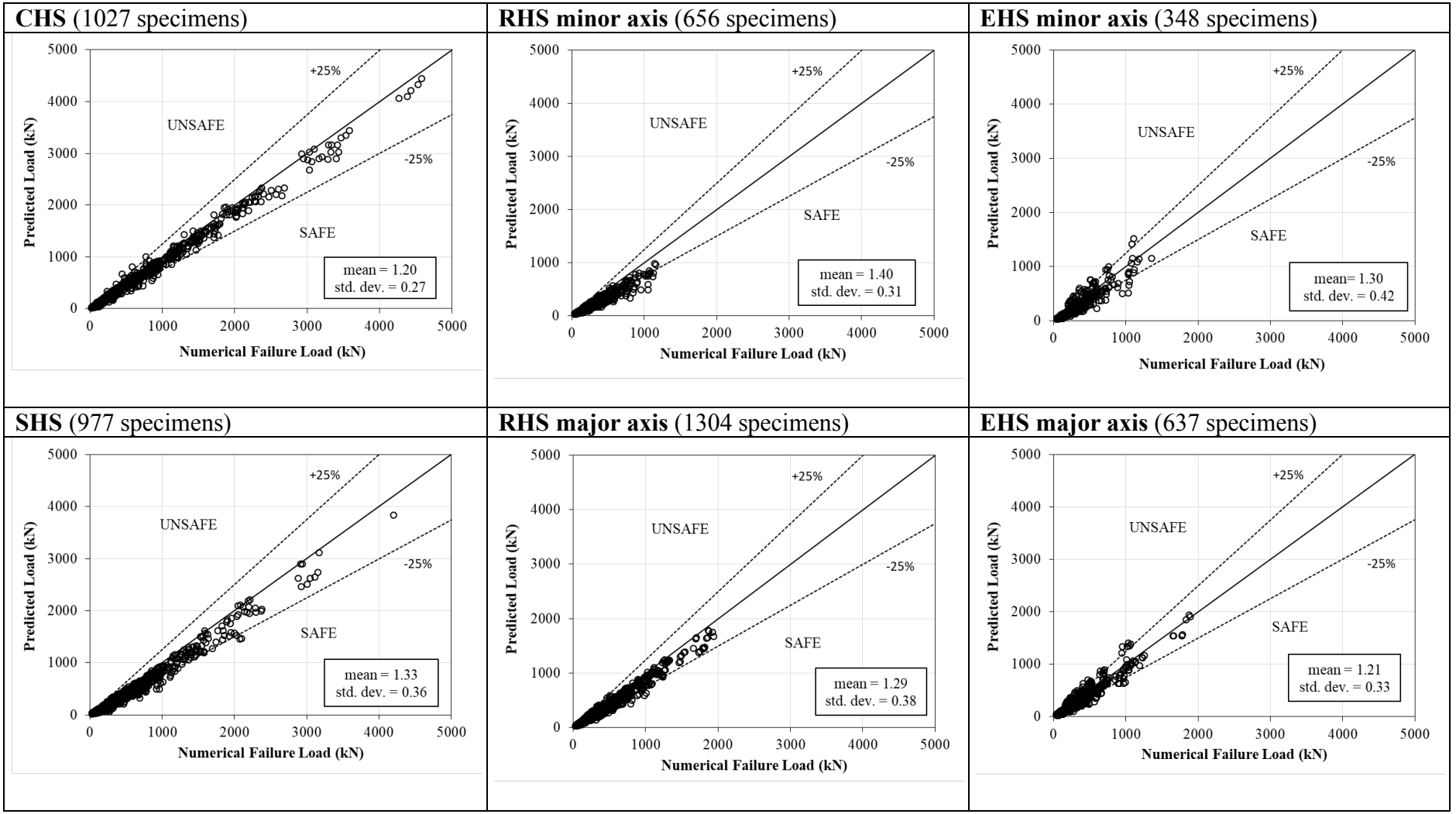


Fig. 6 Comparison of results between numerical parametric study and proposed simplified method, uniform bending moment.

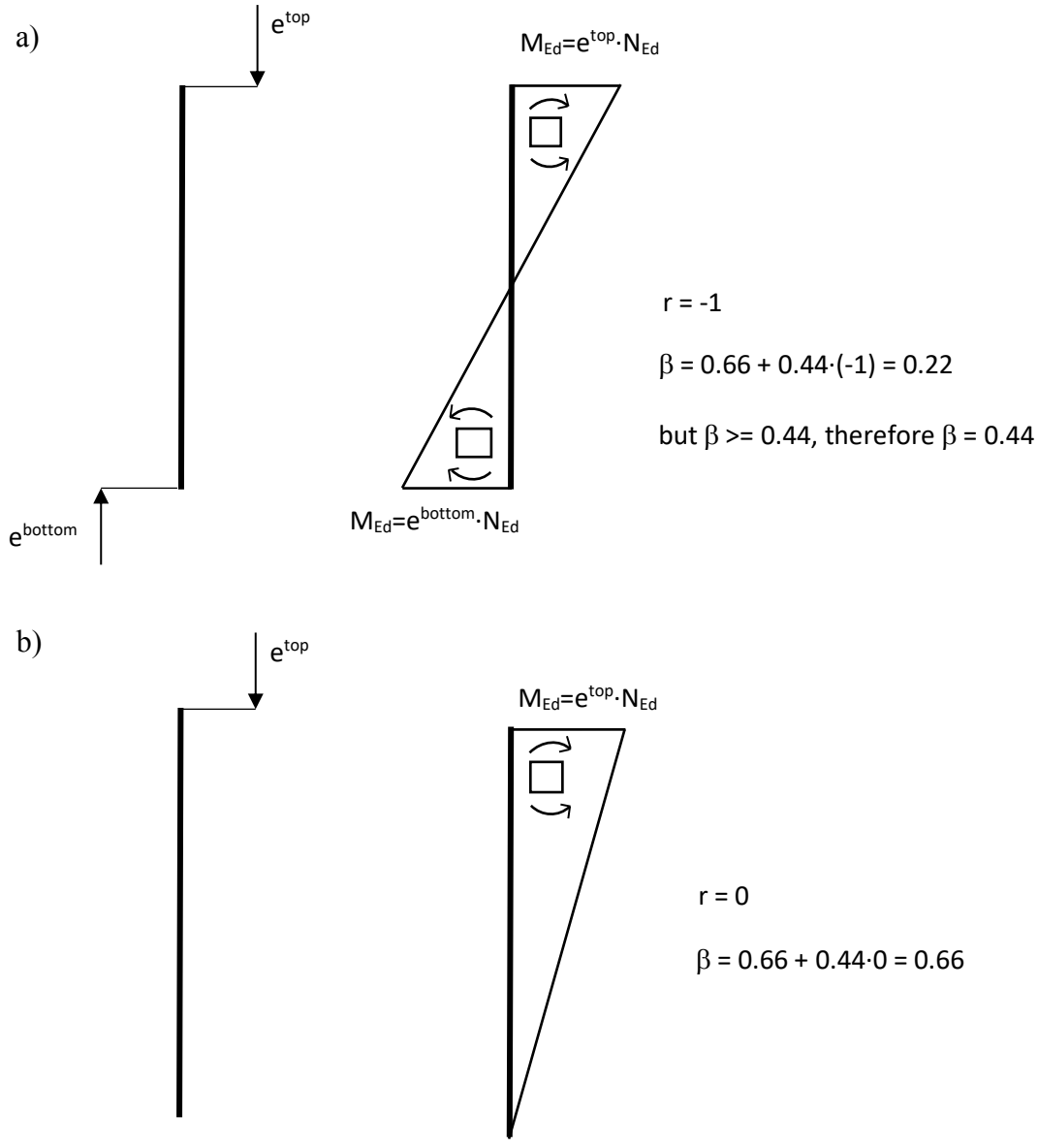


Fig. 7 Variable bending moment diagrams considered: a) $r$ = -1, b) $r$ =0.

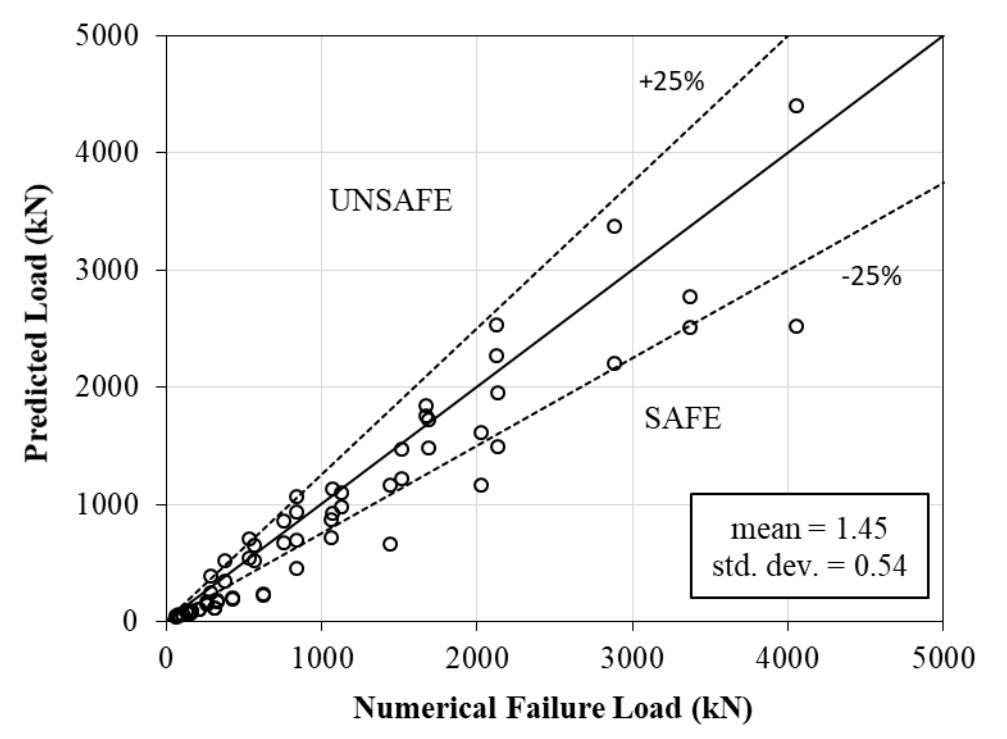


Fig. 8 Comparison of results between numerical parametric study and proposed simplified method, variable bending moment distributions.

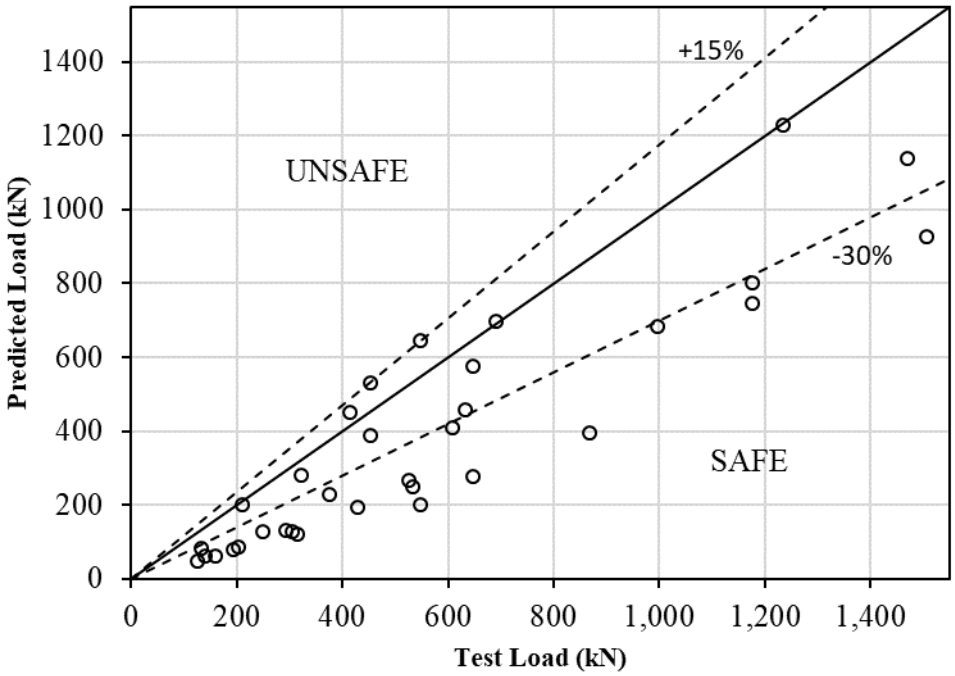


Fig. 9 Comparison against experiments.

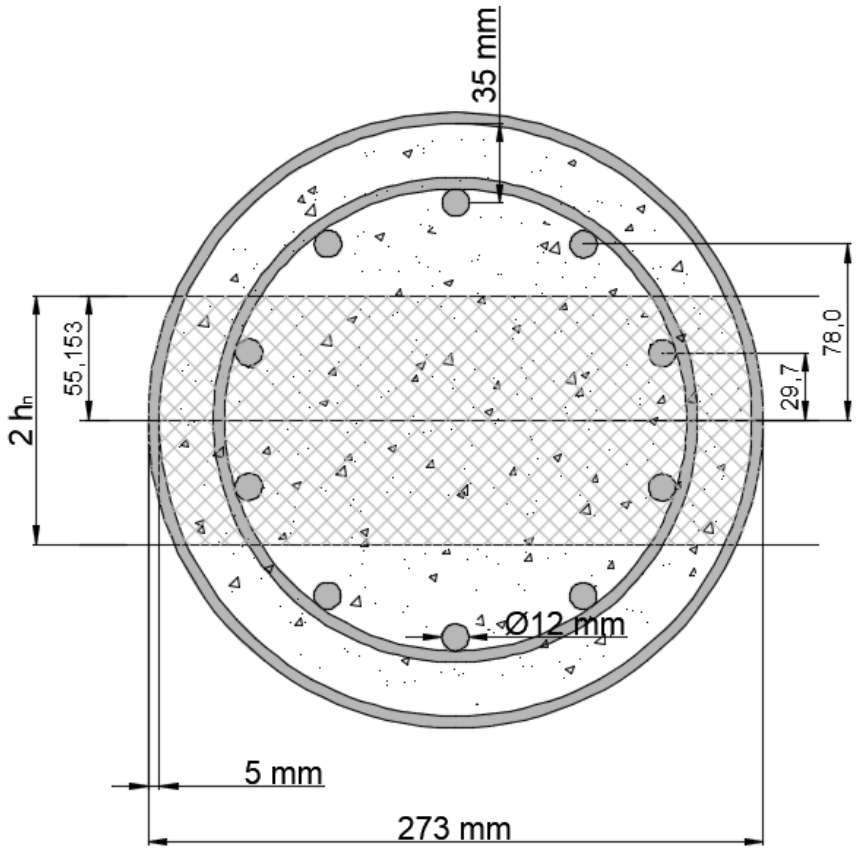


Fig. 10 Cross-section of the column for the worked example.

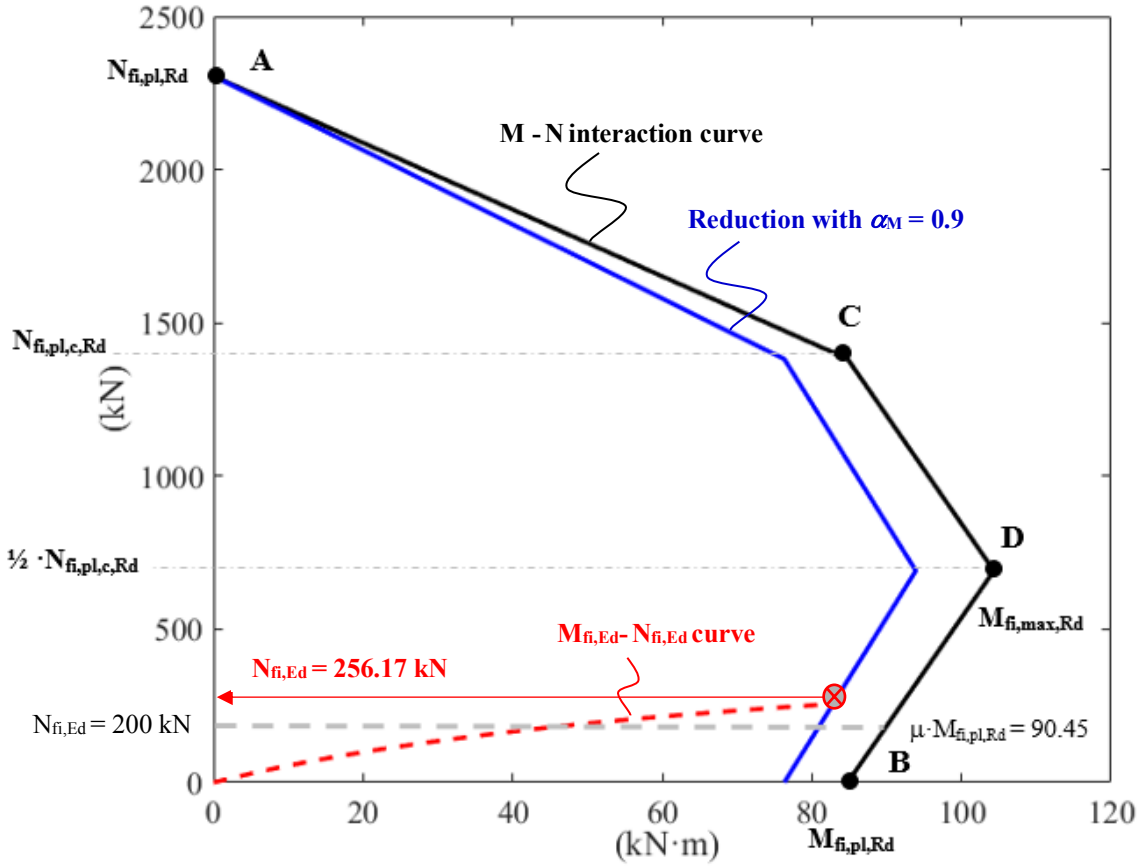


Fig. 11 M-N interaction diagrams for the worked example.

## TABLES

Table 1 Parametric study cases (constant bending moment)

| Section shape | **Circular – CHS** *(1060 analysis cases)* | | | | | | | |
|---|---|---|---|---|---|---|---|---|
| $D$ (mm) | 139.7 | | | 273 | | | 457 | 508 |
| $t$ (mm) | 3 | 12.5 | 5 | 12.5 | | | 8 | 10 |
| $\overline{\lambda}$ | 0.2 - 0.3 - 0.5 - 0.8 - 1 | | | | | | 0.2 - 0.3 - 0.4 - 0.5 - 0.8 - 1 | |

| Section shape | **Square – SHS** *(1037 analysis cases)* | | | | | | | |
|---|---|---|---|---|---|---|---|---|
| $B$ (mm) | 120 | | | 200 | | | 350 | 400 |
| $t$ (mm) | 4 | 12.5 | 6 | 16 | | | 10 | 12 |
| $\overline{\lambda}$ | 0.2 - 0.3 - 0.5 - 0.8 - 1 | | | | | | 0.2 - 0.3 - 0.4 - 0.5 - 0.8 - 1 | |

| Section shape | **Rectangular – RHS** (*1964 analysis cases)* | | | | | | | | | | | |
|---|---|---|---|---|---|---|---|---|---|---|---|---|
| Aspect ratio | **1.5** (1018 *cases*) | | | | **2** (858 *cases*) | | | | **3** (88 *cases*) | | | |
| $H\times B$ (mm) | 150×100 | | 300×200 | | 200×100 | | 400×200 | | 180×60 | | 300×100 | |
| $t$ (mm) | 5 | 10 | 10 | 14.2 | 6 | 12* | 12 | 14.2 | 5* | 10* | 10* | 12.5* |
| $\overline{\lambda}$ (major axis) | 0.2 - 0.3 - 0.5 - 0.8 | | 0.2 - 0.3 - 0.5 - 0.8 | | 0.2 - 0.3 - 0.5 | | | | 0.2 - 0.3 | | | |

| Section shape | **Elliptical – EHS** (*985 analysis cases*) | | | | | |
|---|---|---|---|---|---|---|
| Aspect ratio | **2** | | | | | |
| $H\times B$ (mm) | 220×110 | | 480×240 | | 320×160 | |
| $t$ (mm) | 6.3 | 12.5* | 12.5 | 14.2 | 8 | 14.2 |
| $\overline{\lambda}$ (major axis) | 0.2 – 0.3 – 0.5 – 0.8 – 1 | | | | | |

* Reinforcement not possible because of the minimum rebar spacing requirements from EN 1992-1-1 Section 8.2

Common parameters

| | |
|---|---|
| $\rho$(%) | 0 - 2.5 - 5 |
| $\mu$(%) | 15 - 30 - 45 - 60 for CHS and SHS<br>15 - 30 - 50 - 70 for EHS and RHS |
| $e/D$ (or $e/B$, $e/H$) | 0.25 - 0.5 - 0.75 - 1 |
| *bending axis* | major axis – minor axis |
| $r = e^{bottom}/e^{top}$ | 1 |
| $f_y$ (MPa) | 355 |
| $f_s$ (MPa) | 500 |
| $f_c$ (MPa) | 30 |
| B.C. | P-P |

Table 2 Statistical analysis of results

| | **CHS** | **SHS** | **RHS** | | **EHS** | |
|---|---|---|---|---|---|---|
| | | | minor axis | major axis | minor axis | major axis |
| Average | 1.20 | 1.33 | 1.40 | 1.29 | 1.30 | 1.21 |
| Std. dev. | 0.27 | 0.36 | 0.31 | 0.38 | 0.42 | 0.33 |

Table 3 Parametric study cases for variable bending moment

| **Geometry** | **CHS** (*72 analysis cases*) | | |
|---|---|---|---|
| $D$ (mm) | 139.7 | 508 | |
| $t$ (mm) | 12.5 | 10 | |
| $\overline{\lambda}$ | 0.3 | 0.7 | |
| $\rho$ *(%)* | 0 | 0 | 5 |
| $\mu$ *(%)* | 15 – 30 – 60 | | |
| *e/D* | 0.25 – 0.5 – 0.75 – 1 | | |
| $r = e^{bottom}/e^{top}$ | -1 / 0 | | |
| $f_y$ (MPa) | 355 | | |
| $f_s$ (MPa) | 500 | | |
| $f_c$ (MPa) | 30 | | |
| B.C. | P-P | | |

Table 4 Evaluation of statistical results against CEN/TC250 HGF acceptance criteria

| **Accuracy parameters** | **Result from evaluation** | **HGF [31]** |
|---|---|---|
| Average | 1.75 | > 1 |
| Max. unsafe error | 14.92 % | < 15% |
| No. of unsafe results | 12.12 % | < 20 % |